Signature of microscale kinetics in mesoscale description of epitaxial growth

Joshua P. Schneider and Dionisios Margetis

Phys. Rev. E **96**, 020802 — Published 22 August 2017

DOI: 10.1103/PhysRevE.96.020802

Signature of microscale kinetics in mesoscale description of epitaxial growth

Joshua P. Schneider[1]* and Dionisios Margetis[2]
[1] *Department of Mathematics, University of California, Los Angeles, California 90095, USA*
[2] *Department of Mathematics, and Institute for Physical Science and Technology, and Center for Scientific Computation and Mathematical Modeling, University of Maryland, College Park, Maryland 20742, USA*
(Dated: August 14, 2017)

We describe the effect of *kinetic interactions* of adsorbed atoms in a mesoscale model of epitaxial growth without elasticity. Our goal is to understand how atomic correlations due to kinetics leave their signature in mechanisms governing the motion of crystal line defects (steps) at the nanoscale. We focus on the key atomistic processes related to external material deposition, desorption, and asymmetric energy barriers on a stepped surface. By starting with a kinetic, restricted solid-on-solid model in 1+1 dimensions, we derive laws that govern the motion of a single step when deposition is nearly balanced out by desorption. These mesoscale laws reveal how kinetic processes, e.g. bond breaking at the step edge, influence step motion via the correlated motion of atoms.

PACS numbers: 81.10.Aj, 68.55.-a, 68.35.Md, 64.60.De

Introduction. A fundamental question in statistical physics is the following: How can the erratic motion of atoms give rise to technologically useful structures? This question motivates bottom-up approaches to the modeling of materials, whereby devices are grown or self-assemble from microscale components. A notable example in this vein is the growth of nanowires by the decoration of step edges on vicinal surfaces [1, 2]. In these experiments, the nanowire material is slowly deposited onto a pre-prepared substrate consisting of monatomic line defects (steps) separated by terraces. The adsorbed atoms (adatoms) diffuse on the surface until they attach to step edges. Under suitable experimental conditions, nanowires may then be grown in a controlled way [1, 2].

In this Rapid Communication, we link atomistic and mesoscale models describing such a controlled growth in homoepitaxy. We show how atomic correlations due to kinetics leave their imprint in mesoscale laws for steps.

The kinetic processes leading to nanowire formation at step edges include deposition, adatom hopping with asymmetric energy barriers, and desorption of atoms on the crystal surface [3–6]. The surface morphological evolution can be determined by the motion of individual atoms, e.g., via lattice-gas-type models [7]. However, it is often impractical to completely resolve atomistic details. An alternate description is offered by mesoscale models: Discrete details are retained in the vertical direction of the surface whereas the atomic motion is coarse grained in the lateral directions, in the spirit of the Burton-Cabrera-Frank (BCF) model [8].

In this Rapid Communication, we obtain mesoscale equations of motion via averages of an atomistic, lattice-gas-type model. We find that step flow *is characterized by corrections to the conventional BCF theory* that account for the correlated motion of adatoms due to kinetics. In a suitable regime, these corrections are only controlled by the kinetic rate for bond breaking at the step edge.

To simplify the analysis without losing sight of the essential physics, we limit attention to a single step in one spatial dimension (1D). This setting is consistent with the quasi-one-dimensional geometry of nanowire growth by step decoration [2]. Our model singles out key kinetic processes of crystal surface evolution in 1D below the roughening transition [3]. Hence, we neglect phenomena inherent to geometries in two spatial dimensions (2D) such as nucleation.

The foundation of our work is a high-dimensional master equation describing the transitions between microstates of adatoms in a kinetic, restricted solid-on-solid (KRSOS) model [7, 9, 10]. The time-dependent probability density, $p_{\boldsymbol{\alpha},m}(t)$, defined over KRSOS microstates $(\boldsymbol{\alpha}, m)$, evolves according to

$$\dot{p}_{\boldsymbol{\alpha},m}(t) = \sum_{\boldsymbol{\alpha}',m'} T_{(\boldsymbol{\alpha},m),(\boldsymbol{\alpha}',m')} p_{\boldsymbol{\alpha}',m'}(t) \ . \qquad (1)$$

The symbol $\boldsymbol{\alpha}$ represents the adatom configuration, and the index m measures the mass added to the system; these $\boldsymbol{\alpha}$ and m are independent. In Eq. (1), $T_{(\boldsymbol{\alpha},m),(\boldsymbol{\alpha}',m')}$ is the transition rate from state $(\boldsymbol{\alpha}', m')$ to state $(\boldsymbol{\alpha}, m)$. These rates obey detailed balance, and include external deposition with rate F and desorption with rate τ^{-1}.

We apply Eq. (1) to a single-step geometry, for which $T_{(\boldsymbol{\alpha},m),(\boldsymbol{\alpha}',m')}$ encodes the following kinetic rules [9–11] (see Fig. 1): (a) Atoms that have two in-plane nearest neighbors are immobile; (b) the step-edge atom, which only has one in-plane nearest neighbor, may detach to the upper or lower terrace, becoming an adatom; and (c) adatoms on the terrace do not form bonds with nearest neighbors except at the edge. These rules allow more than one adatom to occupy the same site. By rule (c) islands may not form via bonding of adatoms [10].

We focus on the growth regime in which

$$1 \leq F\tau < (N-1)k \ , \qquad (2)$$

* schneider@math.ucla.edu

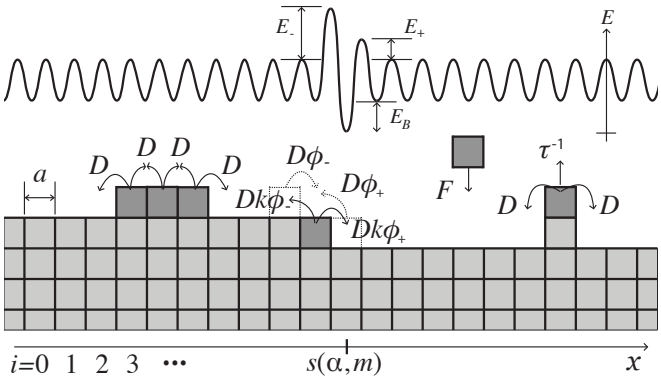

FIG. 1. Schematic for main assumptions of KRSOS model. Bottom panel: Movable atoms are shown in dark grey. The kinetic rates are: D, for atom hopping away from the step; $D\phi_\pm$ (dashed atoms and arrows) for atom attachment to the step from the upper $(-)$ or lower $(+)$ terrace; $Dk\phi_\pm$ for atom detachment or attachment at step; F for deposition from above; and τ^{-1} for desorption. The factors $\phi_\pm = \exp[-E_\pm/(k_BT)]$ account for Ehrlich-Schwoebel barriers, $E_\pm$ [5, 6]. The step position is $s(\boldsymbol{\alpha}, m)$. Top panel: 1D energy-barrier landscape.

where N is an integer expressing the system size ($N \gg 1$), $k = \exp[-E_B/(k_BT)]$, and E_B is the bonding energy of an atom to the step (k_BT is the Boltzmann energy). By condition (2), the number of externally deposited atoms at the desorption time scale is more than one, but is limited by the average number of adatoms detached from the step in equilibrium. We obtain three types of results. First, we describe analytically the stationary solution, $p^{eq}_{\boldsymbol{\alpha},m}$, of Eq. (1); see Eq. (3). This solution describes the KRSOS model in equilibrium. The use of $p^{eq}_{\boldsymbol{\alpha},m}$ along with a "maximum principle" for Eq. (1), outlined below, enable us to estimate the magnitude of corrections to the BCF model. Our approach provides an atomistic view of the interplay between deposition and desorption in regime (2). Second, by *time-dependent* averages over states $(\boldsymbol{\alpha}, m)$, we derive non-equilibrium kinetic laws for the motion of a step; these include corrections to the BCF model. We find that such deviations are controlled by the Arrhenius factor k and the equilibrium adatom density, c^{eq}; see Eqs. (4)–(11). In particular, estimates (11) form a key result of our analysis. Third, we connect our approach to nanowire growth (see Table I).

The present work forms an extension of recent studies in the atomistic origin of crystal growth, e.g., [9–17]. Our specific objectives, however, are different from those of past works. For example, here we explain why neglecting atomic correlations in mesoscale theories such as variants of the BCF model [4] may pose restrictions on atomistic rates. We describe these restrictions, as well as possible implications of their violation in single-step motion.

Our analysis prioritizes *kinetic corrections* to the 1D BCF model, when the system is not at equilibrium, and thus complements [9, 10, 13–15], which focus on the derivation of the standard BCF model (near equilibrium). Our goals resemble those of [16, 17], in which corrections to the BCF model due to nucleation are considered. However, we neglect nucleation here and instead place emphasis on systematic estimates of corrections *due to kinetic interactions when the adatom system is not dilute*. Our approach is distinct from that in [12, 13] where discrete adatom diffusion is speculated without invocation of adatom correlations. The present master-equation approach originated from [10] where deposition and desorption are left out. Our formalism extends the atomistic model of [11] to include desorption. Detailed derivations are omitted here; the interested reader may consult [18].

We use the symbol $\hat{\jmath}$ for a (Lagrangian) lattice site relative to the step, as opposed to the (Eulerian) index j of the fixed lattice. The lattice spacing is denoted by a.

Microscale model. We now elaborate on the KRSOS model; cf. Eq. (1). Following [9–11], we represent each configuration by the ordered pair $(\boldsymbol{\alpha}, m)$; the *multiset* $\boldsymbol{\alpha}$ is an unordered list of the lattice sites that contain adatoms. For example, the state $(\boldsymbol{\alpha}, m) = (\{\}, m_0)$ has no adatoms and an *initial* total number of atoms equal to m_0. The state $(\boldsymbol{\alpha}, m) = (\{\hat{\imath}, \hat{\imath}, \hat{\jmath}\}, m_0 + 2)$ contains two adatoms at site $\hat{\imath}$ and one at $\hat{\jmath}$, of which two came from external deposition and one detached from the step.

By this formalism, the microscale step position is uniquely determined in a given state $(\boldsymbol{\alpha}, m)$: If the step is initially at site s_0 in the fixed lattice frame, the step position at a later configuration $(\boldsymbol{\alpha}, m)$ is $s(\boldsymbol{\alpha}, m) = s_0 - |\boldsymbol{\alpha}| + m - m_0$. This formula invokes the cardinality of $\boldsymbol{\alpha}$, $|\boldsymbol{\alpha}|$: the total number of adatoms in the given state.

The above system representation along with rules (a)–(c) (see Introduction) can be used to define the transition rates $T_{(\boldsymbol{\alpha},m),(\boldsymbol{\alpha}',m')}$ of Eq. (1). By Fig. 1, this matrix accounts for: atom hopping away from the step (rate D); attachment/detachment at the step (rates $D\phi_\pm$ and $Dk\phi_\pm$); and external deposition as well as desorption (rates F and τ^{-1}). Formulas for $T_{(\boldsymbol{\alpha},m),(\boldsymbol{\alpha}',m')}$ are prescribed accordingly; see [9, 10] for mass conserving KRSOS transitions, and [11] if external deposition is included. For desorption, we define $T_{(\boldsymbol{\alpha},m),(\boldsymbol{\alpha}',m')} = \tau^{-1}$ if $m = m' - 1$ and $|\boldsymbol{\alpha}| = |\boldsymbol{\alpha}'| - 1$ and $|\boldsymbol{\alpha}' \setminus \boldsymbol{\alpha}| = 1$. Note that the multiset difference $\boldsymbol{\alpha} \setminus \boldsymbol{\alpha}'$ contains the elements in $\boldsymbol{\alpha}$ that are not in $\boldsymbol{\alpha}'$, counting multiplicity.

We now outline attributes of Eq. (1) that can be used to quantify corrections to the BCF model. A stationary solution to this equation may or may not exist for long times if $F > 0$. In contrast, for mass-conserving dynamics (if $F = 0$), it was shown [10] that a stationary solution to the master equation always exists since the transition rates satisfy Kolmogorov's criterion [19].

In the present case, a consequence of kinetic regime (2) is the existence of a stationary solution to Eq. (1), viz.,

$$p^{eq}_{\boldsymbol{\alpha},m} = (1-k)^{N-1} k^{|\boldsymbol{\alpha}|} (1-\mathcal{R}) \mathcal{R}^{m-m_0} \ ; \qquad (3)$$

$\mathcal{R} = \frac{F\tau}{(N-1)k}$ is a non-dimensional parameter expressing the relative strength of deposition compared to desorption. Notice that Eq. (3) satisfies the detailed-balance relation $T_{(\boldsymbol{\alpha},m),(\boldsymbol{\alpha}',m')} k^{|\boldsymbol{\alpha}'|} \mathcal{R}^{m'} = T_{(\boldsymbol{\alpha}',m'),(\boldsymbol{\alpha},m)} k^{|\boldsymbol{\alpha}|} \mathcal{R}^{m}$, by leaving out the normalization factor. In other words,

in regime (2), the interplay between mass-non-conserving processes brings about a balance that allows for equilibrium to prevail at long enough times. Formula (3) enables us to quantify the impact of the correlated motion of adatoms at the mesoscale, as discussed below.

In regime (2), Eq. (1) obeys a "maximum principle" [18] which states that if the initial data $p_{\boldsymbol{\alpha},m}(0)$ satisfies $\max_{\boldsymbol{\alpha},m}\{p_{\boldsymbol{\alpha},m}(0)/p^{eq}_{\boldsymbol{\alpha},m}\} \leq C$ with a parameter-independent constant C, then $\max_{\boldsymbol{\alpha},m}\{p_{\boldsymbol{\alpha},m}(t)/p^{eq}_{\boldsymbol{\alpha},m}\} \leq C$. Thus, if the distribution over atomistic configurations is close enough to equilibrium initially, it always remains so. This property is derived by singling out the elements $T_{(\boldsymbol{\alpha},m),(\boldsymbol{\alpha},m)}$ in the summation over $(\boldsymbol{\alpha}',m')$ in Eq. (1) and recalling that $p^{eq}_{\boldsymbol{\alpha},m}$ obeys (1) with zero left-hand side.

Discrete averaging. Next, we make use of the averaging

$$\langle Q\rangle = \sum_{\boldsymbol{\alpha},m} Q(\boldsymbol{\alpha},m)p_{\boldsymbol{\alpha},m}(t) \ , \tag{4}$$

where $Q(\boldsymbol{\alpha},m)$ is any microscale quantity and $p_{\boldsymbol{\alpha},m}(t)$ obeys Eq. (1). For example, for suitable $Q(\boldsymbol{\alpha},m)$, the flux on the right (+) or left (−) of the step is

$$\begin{aligned} J_{\pm}(t) = \pm \sum_{\boldsymbol{\alpha},m} \big[& T_{(\boldsymbol{\alpha}_{\pm},m),(\boldsymbol{\alpha},m)}p_{\boldsymbol{\alpha},m}(t) \\ & - T_{(\boldsymbol{\alpha},m),(\boldsymbol{\alpha}_{\pm},m)}p_{\boldsymbol{\alpha}_{\pm},m}(t)\big] \ ; \end{aligned} \tag{5}$$

$\boldsymbol{\alpha}_{\pm}$ is the adatom state resulting from rightward or leftward detachment at the step.

The *discrete* kinetic laws that we obtain via Eq. (4) at the mesoscale include: (i) a step velocity law; (ii) a condition for the adatom flux at the step; and (iii) a diffusion-like equation for the adatom density. These laws form the core of the BCF model [8]. Laws (ii) and (iii) contain corrections due to the correlated motion of adatoms.

The average step velocity is obtained by differentiating step position, $\varsigma(t) = \langle s(\boldsymbol{\alpha},m)\rangle a$, at time t, in view of Eqs. (1) and (5). The resulting motion law is

$$\dot{\varsigma}(t) = a\left[J_{-}(t) - J_{+}(t)\right] \ , \tag{6}$$

as expected by mass conservation [8].

For case (ii), by manipulating Eq. (5) we obtain [11]

$$J_{\pm}(t) = \mp D\phi_{\pm}a\left[c_{\pm 1}(t) - c^{eq}\right] \mp D\phi_{\pm}af_{\pm}(t) \ , \tag{7}$$

where $c_{\hat{\jmath}}(t)$ is the Lagrangian adatom density $\hat{\jmath}$ lattice sites away from the step, $c_{\hat{\jmath}}(t) = \langle \nu_{\hat{\jmath}}(\boldsymbol{\alpha})\rangle/a$, and $\nu_{\hat{\jmath}}(\boldsymbol{\alpha})$ is the number of adatoms at site $\hat{\jmath}$ for configuration $\boldsymbol{\alpha}$. The equilibrium adatom density, c^{eq}, is calculated via stationary solution (3), and is found to be

$$c^{eq} = \frac{\langle n\rangle}{(N-1)a} = \frac{k/a}{1-k} \ , \tag{8}$$

which is independent of the parameter $\mathcal{R}$, and agrees with the respective result in [10] for conserved dynamics in the dilute limit, if $k \ll 1$. In Eq. (7), the terms $f_{\pm}(t)$ are *corrective fluxes* beyond the BCF model; for example,

$$\begin{aligned} f_{+}(t) = k\Big[c^{eq} + \sum_{\boldsymbol{\alpha},m} \mathbb{1}(\nu_{-1}(\boldsymbol{\alpha}) > 0)p_{\boldsymbol{\alpha},m}(t)/a\Big] \\ - \sum_{\boldsymbol{\alpha},m} \mathbb{1}(\nu_{1}(\boldsymbol{\alpha}) > 1)\nu_{1}(\boldsymbol{\alpha})p_{\boldsymbol{\alpha},m}(t)/a \ , \end{aligned} \tag{9}$$

which comes from the *high occupancy* of lattice sites; the function $\mathbb{1}(\cdot)$ is 1 if its argument is true and 0 otherwise.

For case (iii), we seek an equation of motion for the adatom density. It is convenient to accomplish this task for the Eulerian density, $\rho_j(t) = \langle \nu_{j-s(\boldsymbol{\alpha},m)}(\boldsymbol{\alpha})\rangle/a$. The differentiation of this $\rho_j(t)$ in t and use of Eq. (1) yield

$$\begin{aligned} \dot{\rho}_j(t) = D\Delta_j\rho_j(t) + \frac{F}{(N-1)a} - \frac{1}{\tau}\rho_j(t) \\ - D\Delta_jR_j(t) + \frac{1}{\tau}R_j(t) \ , \end{aligned} \tag{10}$$

for all j away from the step [20], which is a variant of the usual discrete diffusion; Δ_j is the second-order finite-difference operator, viz., $\Delta_j u_j = u_{j-1} - 2u_j + u_{j+1}$. The derivation of Eq. (10) relies on the separation of terms expressing occupancy of lattice sites by two or more adatoms from other contributions to the requisite average. The terms $R_j(t)$ then result as *high-occupancy corrections* to discrete diffusion, which originate from the correlated motion of adatoms; see Fig. 2.

Estimates of corrections. In principle, the corrections $f_{\pm}(t)$ and $R_j(t)$ are negligible when the system is sufficiently dilute [10, 11]. In contrast, these corrective terms may become important when two or more adatoms are on the same terrace with high enough probability; see Fig. 2(b), (c). Therefore, it is meaningful to determine for what values of atomistic parameters the terms $f_{\pm}(t)$ and $R_j(t)$ contribute significantly to the mesoscale laws. By invoking properties of Eq. (1), we obtain the bounds

$$|R_j(t)| \lesssim kc^{eq} \ , \quad |f_{\pm}(t)| \lesssim kc^{eq} \ , \tag{11}$$

provided the system is in growth regime (2). Here, the symbol $\lesssim$ indicates boundedness up to a constant factor that does *not* depend on KRSOS parameters.

Estimates (11) are derived by combining formulas for the corrections $f_{\pm}(t)$ and $R_j(t)$, e.g., Eq. (9), with the "maximum principle" for Eq. (1) and the stationary solution, $p^{eq}_{\boldsymbol{\alpha},m}$, from Eq. (3). Consequently, $f_{\pm}(t)$ and $R_j(t)$ are found to be bounded by time-independent quantities that can be evaluated via our explicit formula for $p^{eq}_{\boldsymbol{\alpha},m}$.

Kinetic Monte Carlo (KMC) simulations confirm estimates (11). In Fig. 3 (bottom panel), we compare the high-occupancy corrections to the discrete diffusion, calculated via KMC simulations, to the value kc^{eq} that enters estimates (11) with unit prefactor. The adatom densities and corresponding corrections shown in Fig. 3 are averages over configurations generated by the usual Bortz-Kalos-Lebowitz algorithm (or "n-fold way") [21].

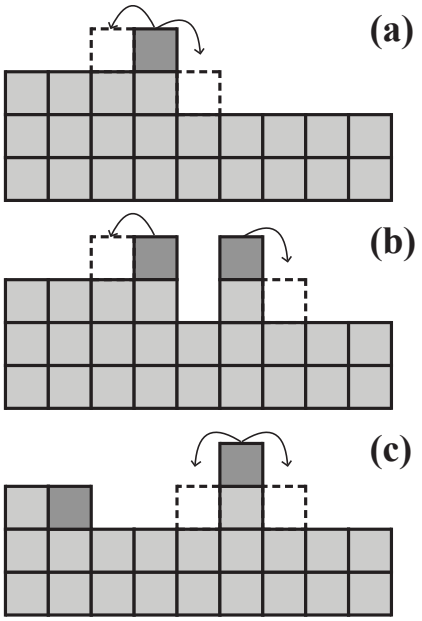

FIG. 2. Illustration of KRSOS configurations in which adatoms interact kinetically with: the step [(a), (b)]; and other adatoms [(c)]. In panel (a), an adatom resting on top of the step atom prevents detachment (yielding a zero detachment rate), but attachment and terrace hopping are still possible. Similarly, no detachment is permitted in panel (b); however, attachment is also forbidden since it would cause the step to advance by more than one lattice site. Panel (c) illustrates that only top-most adatoms in multiply-occupied lattice sites may hop to adjacent sites. Mobile atoms are indicated in dark gray.

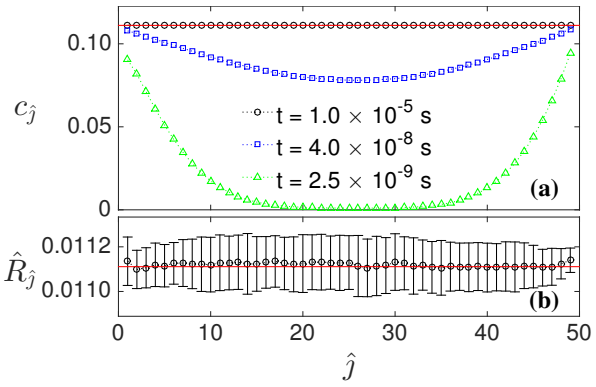

FIG. 3. (Color online) Snapshots of KMC simulations (symbols) for Lagrangian density $c_{\hat{\jmath}}$ and corresponding high occupancy corrections $\hat{R}_{\hat{\jmath}}$. (a) KMC results for $c_{\hat{\jmath}}$ compared to prediction (solid line) for equilibrium density, c^{eq}. (b) KMC results for $\hat{R}_{\hat{\jmath}}$ [the Lagrangian counterpart to $R_j(t)$ appearing in (10)] compared to estimate kc^{eq} for corrections (solid line); cf. (11). Error bars depict the standard deviation of 10 ensembles of 10^5 KMC simulations. Parameters: $N = 50$, $k = 0.1$, $D = 10^{10}$ s^{-1}, $\phi_\pm = 1$, $F = 2 \times 10^7$ atoms/s, and $\tau^{-1} = 10^7$ s^{-1}. These values are typical for KMC simulations in 1D [9].

By estimates (11), the corrections are bounded (up to a constant) by kc^{eq}, which is independent of the deposition and desorption rates, F and τ^{-1}. In contrast, these estimates become *drastically different* if $\tau^{-1} \to 0$ with $F > 0$, when condition (2) ceases to hold: the corrective fluxes and high-occupancy corrections may then strongly depend on F/D, and the Arrhenius factors, $\phi_\pm$, of the Ehrlich-Schwoebel barriers [11]. Estimates (11) indicate that the exchange of atoms with the step (and not the vapor) is the dominant process if inequality (2) holds [11]; thus, the Arrhenius factor k controls $f_\pm(t)$ and $R_j(t)$. This property is a manifestation of the competition between deposition and desorption in kinetic regime (2).

We mention in passing that, in contrast to regime (2), which admits equilibrium distribution (3), master equation (1) can also capture a variety of other, nonequilibrium behavior. If $F \ll \tau^{-1}$ the processes of detachment and desorption cause the step to recede (on average) for long times, as dictated by evaporation. Another regime is $\tau^{-1} \ll F \ll F_c = D(\phi_+ + \phi_-) + (N-1)/\tau$: instead of the equilibrium described by (3), the system evolves toward a nonequilibrium steady state in which the step advances at a finite velocity as $t \to \infty$. When F exceeds F_c, no stationary behavior is possible since step motion is severely hindered by a buildup of adatoms near the step.

Atomistic correlation effects. Next, we discuss the atomistic correlations, illustrated in Fig. 2, which induce corrections $f_\pm(t)$ and $R_j(t)$ in mesoscale motion laws (7) and (10). The corrective fluxes, $f_\pm(t)$, are related to the kinetic rules for detachment and attachment included in the KRSOS model (see Fig. 1). In particular, certain atomistic configurations inhibit detachment and attachment, influencing the adatom flux at the step. Specifically, the fluxes $f_\pm(t)$ are consequences of two types of prohibited transitions: (i) When an adatom is at the site immediately to the left of the step edge, detachment from the step edge is forbidden [Fig. 2(a)]; and (ii) attachment is forbidden if the step would advance by more than one lattice site [Fig. 2(b)]. In both cases, the presence of adatoms near the step edge slightly hinders its motion. This hindrance implies a physically meaningful mechanism of *kinetic interaction* between adatoms and step.

The high-occupancy corrections $R_j(t)$ are related to another type of correlated motion in the KRSOS model. Consider Fig. 2(c), in which two adatoms are at the same lattice site. Only one of the two adatoms may hop to an adjacent lattice site, by the KRSOS rules (Fig. 1). This behavior is attributed to a kinetic interaction between adatoms, which necessitates the appearance of $R_j(t)$ in discrete diffusion. Consequently, adatoms on the terrace are *not subject to conventional Fick's law*; cf. Eq. (10).

In general, corrections to the BCF step flow model due to kinetic interactions are negligible when the system is dilute. Specifically, the configurations in Fig. 2(b)-(c) involve two or more adatoms, which occurs with low probability if the parameters k and F/D are small enough. In contrast, if more than one adatom is present (on average), the corrective fluxes and high-occupancy corrections may

become significant.

Conclusion and discussion. We established that kinetic interactions of adatoms may significantly impact step flow, if both external deposition and desorption are important; see inequality (2). Starting from the 1D KRSOS model of a single step, we isolated the effects of those atomic correlations, which amount to discrete corrections to the adatom flux at the step edge and the diffusion of adatoms on the terrace; cf. Eqs. (7) and (10). The order of magnitude of each correction is $kc^{eq} = k^2/[(1-k)a]$. Hence, for large enough Arrhenius factor k, (i) the fluxes $J_\pm(t)$ may not be linear in the adatom density and (ii) the evolution of the adatom density may be poorly described by the usual diffusion equation.

In the case of the flux at the step edge, Eq. (7), it can be shown [11] that the correction terms, $f_\pm(t)$, can cause deviations from the usual, linear kinetic relation [4]. Figure 3 shows that corrections to adatom diffusion are significant; in particular, corrections measured in those KMC simulations are within 10% of the magnitude of adatom density. On the other hand, our analysis shows that for regime (2), BCF-type step flow can *safely* neglect atomic correlations due to kinetics if $k \ll 1$.

Next, we attempt to connect the above modeling considerations to experimental situations, particularly those of nanowire growth [1, 2]. We aim to describe the regime for which our analysis is valid, particularly estimates (11). We also check whether our corrections to the BCF model can possibly be important in these material systems. A caveat in our present attempt, however, is that we are not aware of the true values for τ^{-1} in [1, 2]. As a compromise, we conservatively assume that $\tau^{-1} \approx 1\ \mathrm{s}^{-1}$. Estimates (11) are valid provided $k > F\tau/(N-1)$, i.e., if k exceeds the external deposition rate (per lattice site). For deposition rate $F = 10^{-3}$, a typical value used in [2], Table I lists the *largest values* of the bonding energy, $E_B^{\max}$, for which the above inequality holds as a function of temperature, T.

T	200	300	400	500
$E_B^{\min}$	0.08	0.12	0.16	0.20
$E_B^{\max}$	0.12	0.18	0.24	0.30

TABLE I. Typical range of bonding energy (eV) for which corrections terms are significant and (11) hold, as a function of temperature (Kelvin); $E_B = -k_B T \log \xi$, where $\xi = k^{\min} \approx 0.01$ for $E_B^{\min}$ and $\xi = F\tau/(N-1) \approx 10^{-3}$ for $E_B^{\max}$.

The values for $E_B^{\max}$ listed in Table I increase if $\tau^{-1} > 1\ \mathrm{s}^{-1}$, and estimates (11) persist. Even if our estimates are valid, it is possible that the corrections terms $R_j(t)$ and $f_\pm(t)$ are negligible, and the usual BCF model is in no need of amendment. Accordingly, we also compute the smallest values of the bonding energies, $E_B^{\min}$, for which correction terms begin to become important, i.e., at least 1% of the size of adatom density or flux; see Table I.

Considering the range of values for bonding energies given in Table I, we notice that for temperatures between 200 K and 500 K, the energy values for which estimates (11) are relevant include the range 0.08 eV–0.3 eV. This range coincides with the kink formation energies for several high-symmetry orientations of Ag and Cu [4]. Here, we make use of the fact that detachment from an 1D step is comparable to detachment from a kink in 2D.

Acknowledgments The authors thank Professors T. L. Einstein and J. D. Weeks for discussions, and acknowledge the support of the National Science Foundation via Grants DMS-1412392 (JPS) and DMS-1412769 (DM).

[1] D. Petrovykh, F. Himpsel, and T. Jung, Surf. Sci. **407**, 189 (1998).
[2] P. Gambardella, M. Blanc, H. Brune, K. Kuhnke, and K. Kern, Phys. Rev. B **61**, 2254 (2000).
[3] A. Pimpinelli and J. Villain, *Physics of crystal growth*, Vol. 53 (Cambridge University Press Cambridge, 1998).
[4] H.-C. Jeong and E. D. Williams, Surf. Sci. Rep. **34**, 171 (1999).
[5] G. Ehrlich and F. Hudda, J. of Chem. Phys. **44**, 1039 (1966).
[6] R. L. Schwoebel and E. J. Shipsey, J. of Appl. Phys. **37**, 3682 (1966).
[7] J. D. Weeks and G. H. Gilmer, Adv. Chem. Phys **40**, 157 (1979).
[8] W.-K. Burton, N. Cabrera, and F. Frank, Phil. Trans. R. Soc. A **243**, 299 (1951).
[9] P. N. Patrone, T. L. Einstein, and D. Margetis, Surf. Sci. **625**, 37 (2014).
[10] P. N. Patrone and D. Margetis, Multiscale Modeling & Simulation **12**, 364 (2014).
[11] J. P. Schneider, P. N. Patrone, and D. Margetis, arXiv preprint arXiv:1606.09272 (2016).
[12] D. M. Ackerman and J. Evans, Multiscale Modeling & Simulation **9**, 59 (2011).
[13] R. Zhao, D. M. Ackerman, and J. W. Evans, Phys. Rev. B **91**, 235441 (2015).
[14] J. Lu, J.-G. Liu, and D. Margetis, Phys. Rev. E **91**, 032403 (2015).
[15] T. Shitara, T. Suzuki, D. Vvedensky, and T. Nishinaga, Appl. Phys. Lett. **62**, 1347 (1993).
[16] A. K. Myers-Beaghton and D. D. Vvedensky, Phys. Rev. B **42**, 5544 (1990).
[17] A. K. Myers-Beaghton and D. D. Vvedensky, Phys. Rev. A **44**, 2457 (1991).
[18] J. P. Schneider, *Multiscale modeling and simulation of stepped crystal surfaces*, Ph.D. thesis, University of Maryland (2016).
[19] The master equation in [10] does not involve the index m, yet it reduces to Eq. (1) provided $F = 0$, $\tau^{-1} = 0$, and $p_{\boldsymbol{\alpha},m}(0) = \delta_{m,m_0} p_{\boldsymbol{\alpha}}(0)$ for some $p_{\boldsymbol{\alpha}}(0)$, where $\delta_{m,m'}$ is Kronecker's delta.
[20] In the vicinity of the step, discrete boundary terms involving fluxes of Eq. (5) enter Eq. (10) [11].
[21] A. B. Bortz, M. H. Kalos, and J. L. Lebowitz, J. Comput. Phys. **17**, 10 (1975).